34th Annual International Conference of the IEEE EMBS
San Diego, California USA, 28 August - 1 September, 2012

Method of Locating Ultrasound-Powered Nerve Stimulators

Daniel W. Gulick, Bruce C. Towe, *Member, IEEE*

Abstract— **We have previously shown a small simple ultrasound-powered nerve stimulator. The piezoelectric implant receives power from an external driving ultrasound transducer. Focusing the ultrasound beam improves power transfer efficiency, but the implant location must be known to aim the focus. We show that currents driven by the stimulator might be detectable on the skin. By scanning the ultrasound focus and measuring the electrical response, we form an image of the implant location. This could give a feedback signal for aiming the beam, and allow multichannel addressing of several stimulators with no added circuitry in the implant.**

I. Introduction

Nerve and brain stimulation is used for a range of medical therapeutics. Most stimulators draw power from an implanted battery, with a lead wire tunneled from the battery to the electrodes at a target tissue. The wire complicates surgery, causes scar tissue, and can break.

Instead of running lead wires, power can be transferred wirelessly through the body. A power driver worn on the skin transmits to a receiver at the stimulation site. The BIONs [1] stimulators show this approach, with inductive power transfer for battery recharging. Another lead-less floating stimulator is the FLAMES [2], which use photovoltaics to receive power from nearby optical fibers. Inductive power is efficient for large receiver coils implanted shallowly in the skin, but less efficient for small deep implants [3]. For implants too small to have an onboard battery like the BIONs do, power transfer efficiency is important for a portable system.

A. Ultrasonic Transcutaneous Energy Transfer (UTET)

Instead of transferring power magnetically between inductive coils, power can also be sent into the body by ultrasound [3, 4]. A transducer on the skin sends ultrasound waves into tissue. The pressure waves create strain on a piezoelectric in the implant. Voltage from the piezoelectric is rectified from a MHz-order frequency into DC power.

The fraction of the beam that does not cross the receiver is wasted, so focusing the power should improve efficiency for small implants. Ozeri et al. [4] described UTET for 100mW-order power levels. This power level requires a relatively large piezoelectric receiver. To keep the local power below the safety limits, it is best to spread the ultrasound beam evenly across the entire piezoelectric receiver. So Ozeri only considers flat unfocused transducers. Denisov and Yeatman [3] also do not appear to consider ultrasound focusing in their analysis of UTET efficiency.

With unfocused ultrasound, power density is typically highest near the skin. Surface heating sets the safety limit for implant power and depth. With focused ultrasound, power density can be higher at the focus (if the focal gain exceeds the attenuation). By compensating for attenuation, focused UTET might allow higher power density at deeper implants.

A difficulty in using focused UTET is aiming the focal spot at the receiver, especially on a moving body. One way to localize the implant would be to add a standard pulse-echo imaging system to the power transmitter, but this would add cost and complexity. Another way to detect ultrasound exciting a piezoelectric implant is to detect the generated electrical current by pickup electrodes on the skin. This technique has been described more generally as a method of creating an ultrasound contrast agent or position marker for implants, using a conventional imaging system [5]. When the ultrasound beam excites the piezoelectric, high frequency currents are capacitively driven into tissue. The detected electrical signals can be used to find the depth and location using the transit time and beam angle.

B. Ultrasound-Powered Nerve Stimulator

We have shown an implantable nerve cuff stimulator powered by a small (1 mm^3) PZT element at safe ultrasound levels [6]. This stimulator contains only the piezoelectric ceramic, a diode, a charge-balancing capacitor, and platinum electrodes (fig. 1). The piezoelectric converts applied ultrasound to MHz voltage, which is half-wave rectified by the diode then passed directly to tissue by the electrodes. No smoothing is done since the nerve responds to the DC average of the current and ignores the superimposed MHz currents.

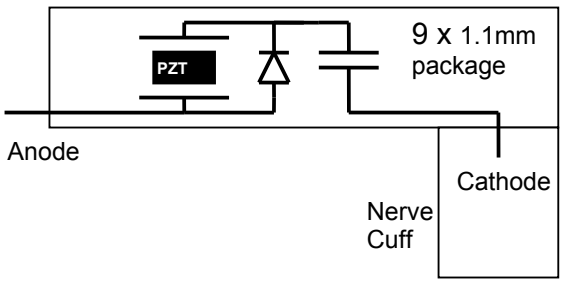

Fig. 1. Diagram of ultrasound-powered nerve stimulator [6].

In this work using the same stimulator we show that the MHz currents should be detectable on the skin. Incidentally to its function, the stimulator also acts as a position marker. The amplitude of the MHz signal on the skin is proportional

Manuscript received March 29, 2012. Work was supported by ASU and National Institutes of Health grants R21-EB003464, R21-NS063213.

Daniel W. Gulick and Bruce C. Towe (corresponding author) are with the School of Health and Biological Systems Engineering, Arizona State University, Tempe, AZ 85287 USA.

to the overlap of the ultrasound beam with the piezoelectric location. As the beam sweeps over an area, the direction that returns the largest signal shows the implant position. This measurement could be repeated as a feedback signal in order to maintain a power link despite movements of the exciter with respect to the implant. With a narrow beam, nearby stimulators might be powered and controlled independently.

II. Background

A. Ultrasound Focusing

The width of the smallest achievable focal zone is inversely proportional to the ultrasound frequency. Shorter wavelengths can be focused more tightly. This gives more focal gain, improving the efficiency. However, high frequencies also lose more power in transmission since the attenuation constant increases linearly with frequency.

There is no need to have a focal spot smaller than the implant, but above this limit the optimum frequency will have a tradeoff depending on implant depth.

B. Volume Conduction

Volume conducted electrical currents in the body could be used for both power and communication. This method sends signals from implanted electrodes to electrodes on the body surface [7]. For a short dipole driving current in uniform volume conductor, the potential Φ at a distant measurement point can be approximated [8]

$$\phi = i\,D \times \frac{\cos(\theta)}{4\,\pi\,\sigma\,r^2}$$

where i is the dipole current, D is dipole length, r is distance to the point, σ is the medium conductivity, and θ is the difference in orientation between the dipole vector and the vector from the dipole center to the measurement point. To estimate the voltage between differential electrodes on the body surface, we take the difference between two potentials as shown in fig. 2.

As an example calculation we use a dipole current of 1 mA, dipole length 1 cm, receiver separation 2 cm, and implant depth 5 cm. The receiver dipole vector is aligned parallel to the implant dipole. In muscle tissue at 1MHz, impedance is approximately 0.5 S/m [9]. These values return a potential difference of 250 μV, which should be detectable by low-noise differential amplifier.

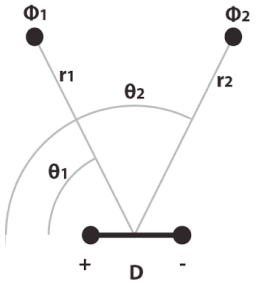

Fig. 2. Source and receiver dipole arrangement for approximating attenuation of volume conducted currents. In the proposed system, the stimulator acts as a dipole transmitting to skin surface electrodes.

The strategy proposed by this work is to use short ultrasound pulses to evoke a locating electrical response from implanted devices. Low-power microsecond-order current pulses do not stimulate tissue. Once the implanted devices have been located and targeted then a longer ultrasound pulse could be emitted to drive stimulation.

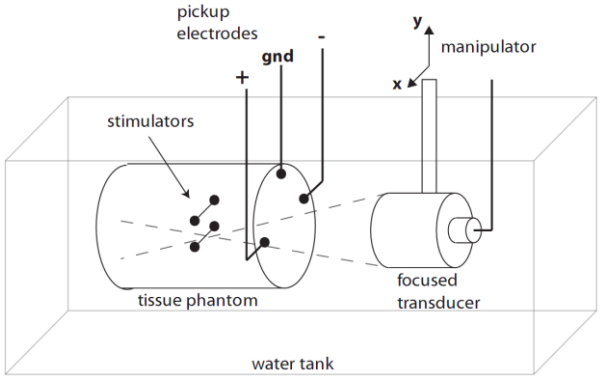

Fig. 3 Setup for finding the stimulator position from the volume-conducted response. As the ultrasound focus is swept through the phantom, the stimulators drive varying levels of current to the pickups depending on how much of the beam is intercepted.

III. Methods

The experimental setup is diagrammed in fig. 3, and the signal path is traced in fig 4. The transducer emits pulses of ultrasound, which are received by the stimulators. The stimulators drive pulses of half-wave rectified current, which are received by the electrodes. The manipulator scans the ultrasound focus across through a tissue phantom. Responses measured at each x/y transducer position are compiled to form a map of the stimulator position in the implant.

Pork tissue obtained from market sources was immersed in saline employed as a coupling medium for the ultrasound. This setup was used as a tissue phantom to model the acoustic (attenuation and scattering) and electrical (impedance) properties of an implant environment. The two stimulators lay side-by-side, 5 mm apart, between layers of pork 2.8 cm deep from the front surface of the phantom. The piezoelectric neurostimulator is described in more detail by Larson et al.[6].

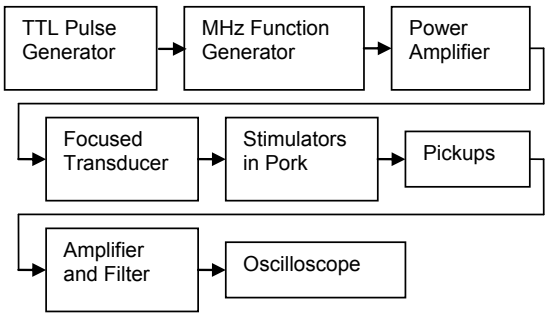

Fig. 4. Signal path for the mapping system

The differential pickup and reference electrodes (silver / silver-chloride) were placed on the front face of the phantom. The pickup electrodes lie on a dipole axis parallel to the stimulators since this orientation gives the largest signal.

We use a laboratory-built 1 MHz transducer (50x2.1 mm PZT-4, Steiner & Martins Inc, Miami FL) with a cast epoxy focusing lens. The beam intensity profile is mapped in fig. 5 by hydrophone (Precision Acoustics, Dorsey UK). The power amplifier is a laboratory-built square-wave driver [10].

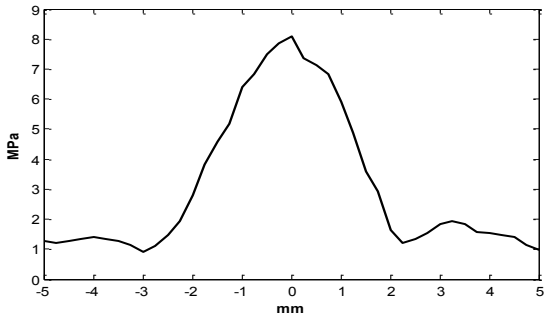

Fig. 5. Temporal-peak pressure across the focus of the ultrasound beam

The transducer is mounted on a 3-axis manipulator. Axial distance from the transducer to the stimulator is fixed at the focal distance (6.5cm), only lateral adjustments are used in the experiment. The focus is swept across a 1 cm^2 region in 1 mm steps.

The pickup differential amplifier is blanked for 40us from the start of the pulse. This prevents overload by artifact from the transducer drive and ringdown. Received signals are amplified and bandpass filtered from 300kHz to 5MHz.

IV. Results

Fig. 6 plots an example of the received signal, volume-conducted from the stimulators to the pickups. The 40µs transit time corresponds to the 65 mm transducer-to-implant distance, at 1500 m/s (approximate speed of sound in water and tissue). Signals past 60 µs show reflections off the sides or ends of the phantom.

As the manipulator scans the focus through the phantom, peak-to-peak voltage is measured at each position. The response along a 1 cm sweep through the center of the phantom is shown in fig. 7. The two peaks occur 6 mm apart, which closely matches the true 5 mm spacing between the stimulators. The width of the peaks matches the beam profile from fig. 5. The response curve can be seen as a convolution of the beam with the implant positions.

The response across the entire 1 cm^2 region is mapped in figure 8. The peaks correspond to the position of the two piezoelectric receivers in the phantom

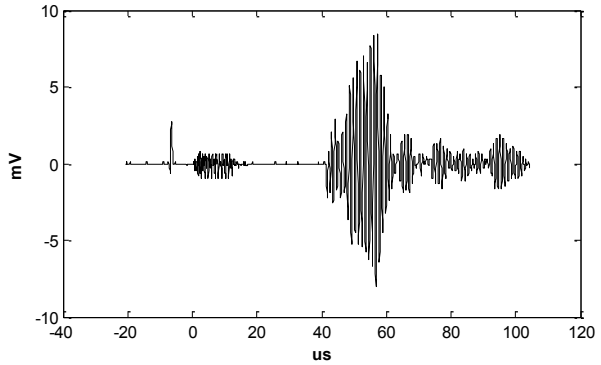

Fig. 6. Waveform of the stimulator current as received by the pickup electrodes. 0 to 10 µs shows the transducer artifact. Amplifier blanking stops at 40 µs. 50 to 60 µs shows the response as the wave passes through the piezoelectric and is converted to current.

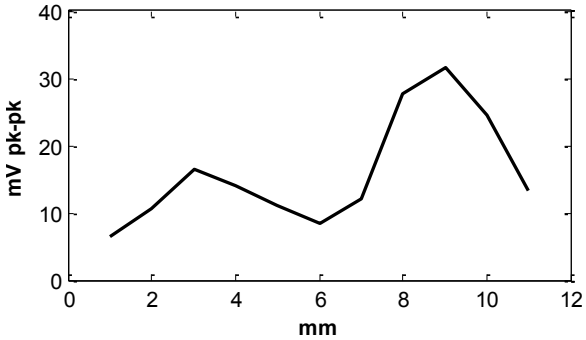

Fig. 7. Response of the stimulator as it varies with transducer position. Extracted from the peak-to-peak voltage of the waveforms as shown in fig. 5.

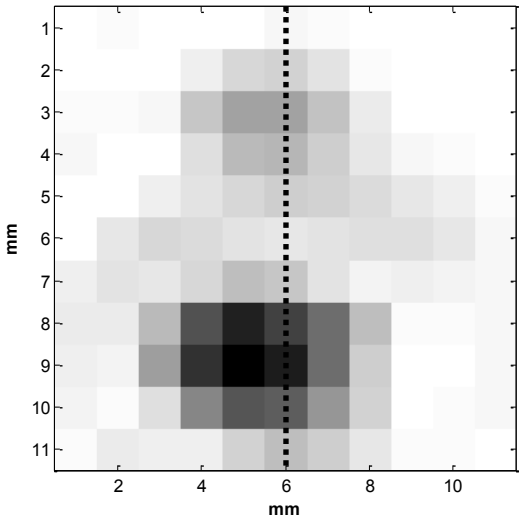

Fig. 8 Map of received voltage as a function of transducer position. Peaks show when the ultrasound focus overlaps with one of the two stimulator locations. Voltage along the dashed line is plotted in fig. 6.

V. Discussion

The ability to resolve the two stimulators suggests they could be separately targeted and powered. Stimulation intensity and duration would be directly set by the ultrasound beam power and dwell time.

The system presently cannot predict the stimulation current. The attenuation through tissue is generally unknown, so the power received by the stimulator is unknown. We previously reported a technique of pulse width modulation that is a possible approach to calibrating power values [11].

The time-peak spatial-peak intensity used in this work was 8 MPa as a proof of concept with a very simple receiving and demodulating system. Peak-to-peak voltage is a noise-sensitive measurement which inefficiently uses the received power. Still, volume conducted signals do have high attenuation in the body [7]; this is a limiting factor for short devices with small dipole moments.

Ultrasound powered neurostimulators of our reported design are particularly suited for this method since their function directly emits a high frequency signal with no waveform smoothing. MHz frequency signals are above 60 Hz and other environmental noises and so may be more easily detected than simple pulse waveforms. Thus we detect the signal mostly at the drive frequency (1MHz), but one could also detect the DC component of the stimulation pulse, or separately filter the harmonics (2MHz, 3MHz, etc) made by the diode.

The system would be implemented with a phased array transducer rather than a fixed focus. The focus of a phased array can be electronically swept and varied in depth. With this flexibility, more efficient aiming and feedback techniques may be possible [12].

The passive multichannel addressing described could be used for simple ultrasound-powered biopotential recorders [13]. These recorders are nearly identical to the stimulators (containing only a piezoelectric, a diode, and electrodes), and work by using the diode as an AM mixer to encode the electrode offset voltage onto the received ultrasound wave.

VI. Conclusion

Focusing and scanning of an interrogating ultrasound beam through tissue and then detecting evoked skin potentials shows promise as a way of locating and independently powering ultrasound powered neurostimulators so as to achieve multichannel operation.

References

[1] G.E. Loeb, R.A. Peck, W.H. Moore and K. Hood, "BION™ system for distr. neural prosthetics," Med. Eng. Phys., vol. 23, pp. 9-18, 2001

[2] A. Abdo, M. Sahin, D.S. Freedman, E. Cevik, P.S. Spuhler, M.S. Unlu. "Intraspinal stimulation with light activated micro-stimulators," Neural Engineering (NER), 2011 5th International IEEE/EMBS Conference on , vol., no., pp.546-549, April 27 2011-May 1 2011

[3] A. Denisov and E. Yeatman, "Ultrasonic vs. inductive power delivery for miniature biomedical implants," 2010 International Conference on Body Sensor Networks (BSN), p. 84, 2010.

[4] S. Ozeri and D. Shmilovitz, "Ultrasonic transcutaneous energy transfer for powering implants," Ultrasonics, vol. 50, p. 556, 2010.

[5] B.C. Towe, "Piezoelectric contrast materials for ultrasound imaging," *Ultrasonics, Ferroelectrics and Frequency Control, IEEE Transactions on* , vol.52, no.9, pp.1483-1488, Sept. 2005

[6] P.J. Larson, B.C. Towe, "Miniature ultrasonically powered wireless nerve cuff stimulator," Neural Engineering (NER), 2011 5th International IEEE/EMBS Conference on , vol., no., pp.265-268, April 27 2011-May 1 2011

[7] D.P. Lindsey, E.L. McKee, M.L. Hull, S.M. Howell, "A new technique for transmission of signals from implantable transducers," *Biomedical Engineering, IEEE Transactions on* , vol.45, no.5, pp.614-619, May 1998

[8] R. Plonsey and R.C. Barr, 2007 *Bioelectricity—A Quantitative Approach* 3rd ed. (New York: Springer) pp 33

[9] S. Gabriel, R.W. Lau, C. Gabriel: "The dielectric properties of biological tissues: II. Measurements in the frequency range 10 Hz to 20 GHz", Phys. Med. Biol. 41 (1996), 2251-2269.

[10] G.K. Lewis, W.L. Olbricht, "Design and characterization of a high-power ultrasound driver with ultralow-output impedance," Review of Scientific Instruments , vol.80, no.11, pp.114704-114704-8, Nov 2009

[11] D.W. Gulick, B.C. Towe. Modeling wireless control of a single-diode neurostimulator. Program No. 520.25. 2011 Neuroscience Meeting Planner. Washington D.C: Society for Neuroscience, 2011. Online.

[12] N.P. Willis, A.F. Brisken, M.W. Cowan, M. Pare, R. Fowler, J. Brennan. "Optimizing energy transmission is a leadless tissue stimulating system", U.S. Patent 0294208, Nov. 27, 2008.

[13] B.C. Towe, P.J. Larson, D.W. Gulick, "Wireless ultrasound-powered biotelemetry for implants," Engineering in Medicine and Biology Society, 2009. EMBC 2009. Annual International Conference of the IEEE , vol., no., pp.5421-5424, 3-6 Sept. 2009